Ye et al. Nanoscale Research Letters (2015) 10:454
DOI 10.1186/s11671-015-1161-3

Nanoscale Research Letters
a SpringerOpen Journal

NANO EXPRESS Open Access

A Facile Way to Fabricate High-Performance Solution-Processed n-MoS_2/p-MoS_2 Bilayer Photodetectors

Jian Ye[1*], Xueliang Li[2], Jianjun Zhao[1], Xuelan Mei[1] and Qian Li[1]

Abstract

Two-dimensional (2D) material has many advantages including high carrier mobilities and conductivity, high optical transparency, excellent mechanical flexibility, and chemical stability, which made 2D material an ideal material for various optoelectronic devices. Here, we developed a facile method of preparing MoS_2 nanosheets followed by a facile liquid exfoliation method via ethyl cellulose-assisted doping and utilizing a plasma-induced p-doping approach to generate *t* effectively the partially oxided MoS_2 (p-MoS_2) nanosheets from the pristine n-type nanosheets. Moreover, an n-p junction type MoS_2 photodetector device with the built-in potentials to separate the photogenerated charges is able to significantly improved visible light response. We have fabricated photodetector devices consisting of a vertically stacked indium tin oxide (ITO)/pristine n-type MoS_2 nanosheets/p-MoS_2/Ag structure, which exhibit reasonably good performance illumination, as well as high current values in the range of visible wavelength from 350 to 600 nm. We believe that this work provides important scientific insights for photoelectric response properties of emerging atomically layered 2D materials for photovoltaic and other optoelectronic applications.

Keywords: Liquid exfoliation method, Partially oxided MoS_2, Photodetectors

Background

Over the last decade, two-dimensional (2D) nanomaterials have drawn great attention because of their unique structures, large natural abundance, and distinctive properties compared to their bulk forms, and a broad range of applications in catalysis, electronics, energy-storage devices, optoelectronics, and so on [1–11]. In particular, the semiconducting layered transition metal dichalcogenides (LTMDs, e.g., WSe_2, WS_2, and MoS_2) have gained significant interest on optoelectronics due to their direct bandgaps, possessing intriguing optical properties suitable for optoelectronic applications in light-emitting diodes and photovoltaics [12–14]. Usually, LTMDs have a unique 2D X–M–X structure in which the transition metal atom layer is sandwiched between two close-packed chalcogen atom layers [1, 2, 15–17].

As a prototypical compound of LTMDs, MoS_2 has been extensively studied. Bulk MoS_2 is a typical semiconductor with an indirect bandgap. Expectedly, monolayer MoS_2 transistors have been demonstrated with on/off ratios of 10^8 and ultralow standby power dissipation [17–19]. However, to realize the highly efficient optoelectronic devices based on MoS_2, it is also important to develop a strategy to prepare ultrathin MoS_2 nanosheets and tune the bandgaps with facile process. Several methods, such as mechanical exfoliation (the so-called Scotch tape method), liquid exfoliation, colloidal synthesis, chemical vapor deposition, chemical exfoliation, and electrochemical exfoliation have been developed to prepare ultrathin MoS_2 nanosheets [2, 20–30]. Among these methods, liquid exfoliation not only produces novel materials with the same composition yet dramatically changed electrical properties but also provides a facile way to prepare thin-layer nanosheets, which offers novel opportunities in the optoelectronics applications [17, 31–34].

In this work, we report that a novel liquid exfoliation method via ethyl cellulose-assisted doping can prepare an

* Correspondence: bbyejian@126.com
[1]Department of Chemistry and Environmental Engineering, Bengbu College, Bengbu, Anhui 233030, China
Full list of author information is available at the end of the article

excellent thin MoS_2 nanosheets and very effective method to generate the partially oxidized MoS_2 (p-MoS_2) nanosheets from the pristine n-type nanosheets. Moreover, an n-p junction type MoS_2 photodetector device with the built-in potentials to separate the photogenerated charges can result in significantly improved visible light response. We have fabricated photodetector devices consisting of a vertically stacked indium tin oxide (ITO)/pristine n-type MoS_2 nanosheets/p-MoS_2/Ag structure, which exhibit reasonably good performance illumination, as well as high current values in the range of visible wavelength from 350 to 600 nm. This work provides important scientific insights for leveraging unique optoelectronic properties of 2D materials for photodetector applications.

Methods

Material Synthesis

Molybdenum disulfide (MoS_2) nanosheets were synthesized by liquid ultrasound exfoliation as reported in the literature [35, 36]. Typically, MoS_2 power (0.25 g, Aladdin) was dispersed in ethyl cellulose (EC) isopropanol solution (1 % *w*/*v* dispersion, 100 ml) in a SEBC bottle. The dispersion was sonicated for 24 h at 60 W in water bath. The resulting dispersion was centrifuged (Desktop High-speed Refrigerated Centrifuge Model TGL-16) at 5000 rpm for 15 min, and then the supernatant liquid was directly collected. Deionized water was mixed with the supernatant liquid (3:4 weight ratio) and subsequently centrifuged at 7500 rpm for 10 min. Whereafter, the lower precipitation was collected and dried. The resulting precipitation was redispersed in ethanol (10 mg/ml). NaCl aqueous solution (0.04 g/ml) was mixed with the redispersion (9:16 weight ratio) and centrifuged at 5000 rpm for 8 min, discarding the supernatant. To debride any residual salt, the resulting MoS_2 precipitation was washed with deionized water and collected by vacuum filtration (0.45 μm filter paper). Finally, the MoS_2 nanosheet product was dried as a fine black powder. The final MoS_2 nanosheets were defined as n-MoS_2. For the preparation of p-MoS_2 nanosheets, the n-MoS_2 powder was taken a UV-ozone plasma treatment for 40 min to completely change to p-MoS_2 nanosheets.

Characterizations

TEM images were taken by a FEI TECNAI G2 F20-TWIN TEM. Raman spectra were recorded on inVia Raman microscope. XPS and UPS measurements were conducted using an ESCALAB 250Xi (Thermo) system. X-ray diffraction (XRD) patterns of the MoS_2 was carried out on a Bruker D8 Focus X-ray diffractometer operating at 30 kV and 20 mA with a copper target (λ= 1.54 Å) and at a scanning rate of 1°/min.

Photodetector Device Fabrication

All devices were fabricated on pre-treatment ITO glass substrates [37] (sheet resistance <10 Ωsq^{-1}, ShenZhen NanBo Display Technology Co., Ltd.); cleaned sequentially using sonication in acetone, detergent, deionized water, and isopropanol; and then dried under a nitrogen stream, followed by ultraviolet light irradiation. Then, the n-MoS_2 nanosheets (10 mg/ml, in isopropanol) spin coated with 2000 rpm and thermally annealed at 150 °C for 15 min receive a thickness of 80 nm. Thereafter, the p-MoS_2 nanosheets (15 mg/ml, in isopropanol) was spin coated on n-MoS_2 nanosheets layer, followed by thermal annealing at 150 °C for 10 min in atmospheric environment. Eventually, Argentum Ag (150 nm) was deposited over the p-MoS_2 nanosheets layer by thermal

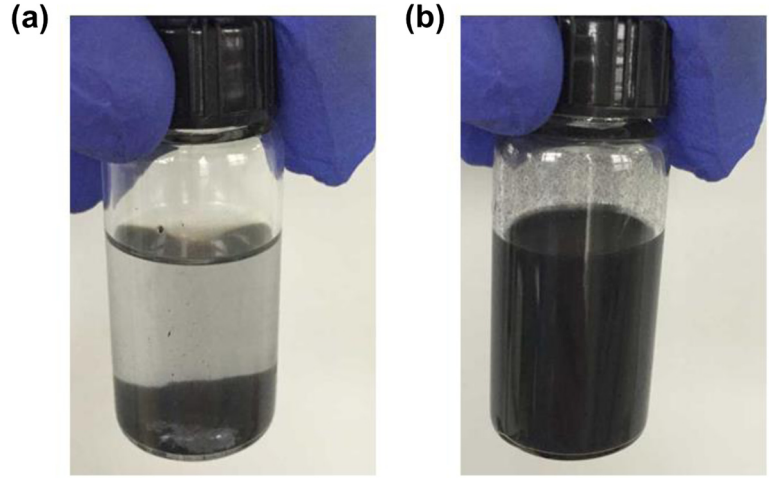

Fig. 1 The images are camera pictures of **a** pristine MoS_2 and **b** MoS_2 nanosheets dispersion

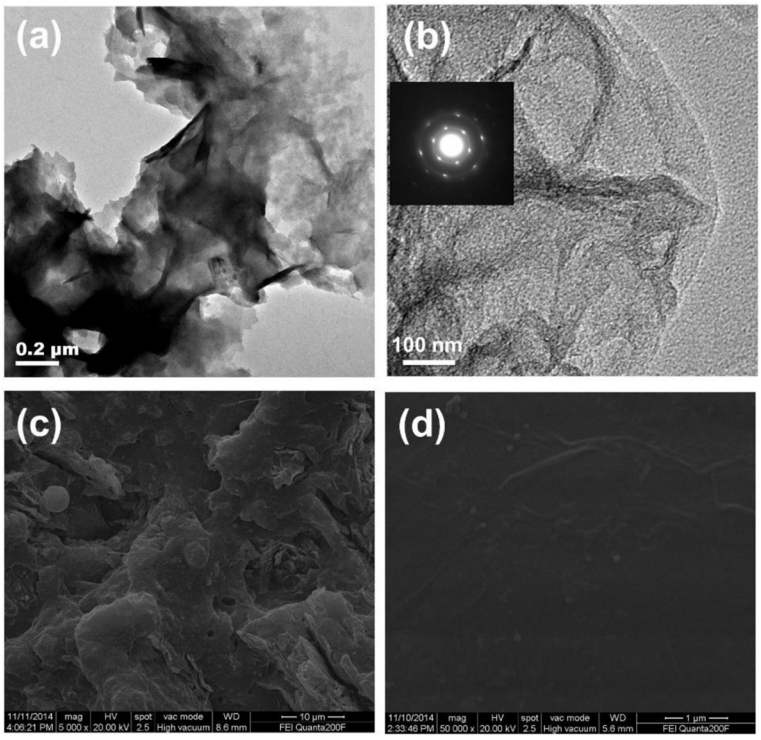

Fig. 2 The transmission electron microscopy (TEM) images of **a** pristine MoS_2 and **b** MoS_2 nanosheets films on glass substrate, and the *inset* is selected area electron diffraction (SAED) pattern of the MoS_2 nanosheets. The scanning electron microscopy (SEM) images of **c** pristine MoS_2 and **d** MoS_2 nanosheets films on glass substrate

evaporation under a vacuum of 6×10^{-6} Torr to accomplish the device fabrication. The effective area of one cell was ~1 cm^2. The photocurrent-voltage curves and I-T curves were measured with a Keithley 2400 source meter and a 150-W Xe lamp light source. The dark current-voltage curves were measured by Keithley 2400 source meter under dark. All the measurements were performed under ambient atmosphere at room temperature. The incident photo-to-electron conversion efficiency spectrum (IPCE) were detected under monochromatic illumination (Oriel Cornerstone 260 1/4 m monochromator equipped with Oriel 70613NS QTH lamp), and the calibration of the incident light was performed with a monocrystalline silicon diode.

Results and Discussion

The equal concentration of pristine MoS_2 and MoS_2 nanosheets after the liquid ultrasound exfoliation solution

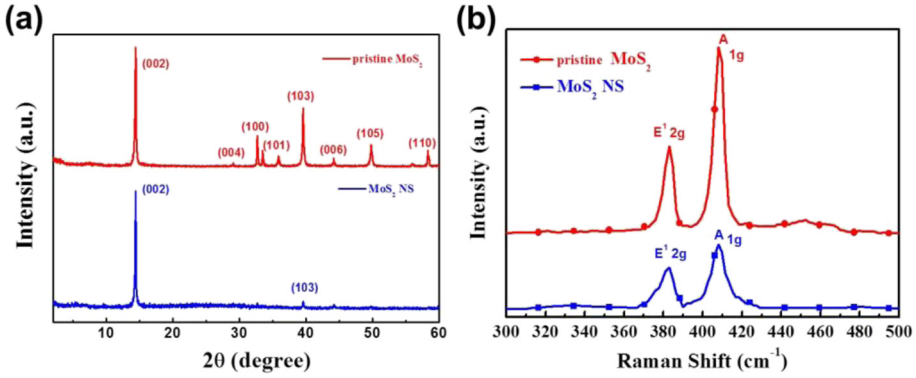

Fig. 3 **a** XRD patterns of the MoS_2 films on glass substrate. **b** Raman spectrum of MoS_2 films on glass substrate

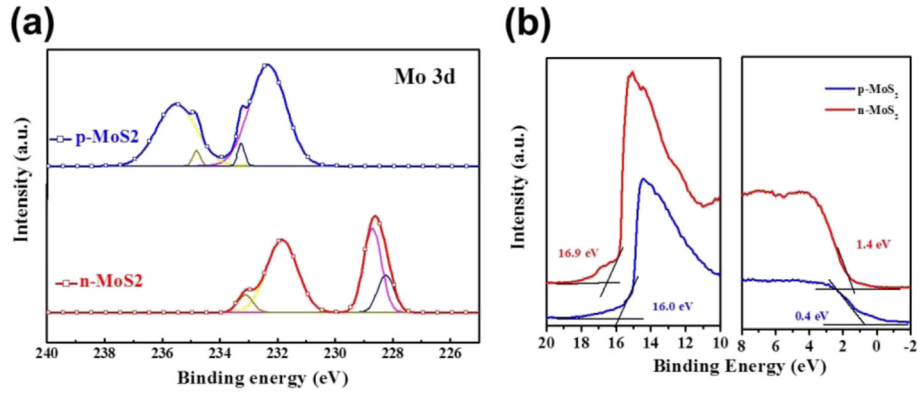

Fig. 4 a Mo 3D region and of X-ray photoelectron spectroscopy (XPS) profiles of MoS_2 nanosheets with or without plasma treatment. **b** The ultraviolet photoelectron spectroscopy (UPS) spectra of MoS_2 nanosheets with or without plasma treatment

(10 mg/ml) was treated with ultrasound in ethanol for 30 min, respectively. The detailed process is demonstrated in experimental section. The photographs of pristine MoS_2 and MoS_2 nanosheets isopropanol dispersion solutions after ultrasound treatment are shown in Fig. 1. After storing for 48 h, humorous aggregation can be observed in pristine MoS_2 solution (Fig. 1a) and evident MoS_2 particles adhere to the sidewall. In contrast, the MoS_2 nanosheets after the liquid ultrasound exfoliation solution show a highly uniform and homogeneous suspension solution (Fig. 1b), indicating the successful preparation of MoS_2 nanosheets with the good dispensability.

In order to verify the degree of dispersion of exfoliated MoS_2 nanosheets by ethyl cellulose ethanol solution via liquid ultrasound exfoliation, transmission electron microscopy (TEM) and scanning electron microscopy (SEM) were performed (Fig. 2). For comparison, the morphologies of the pristine MoS_2 nanosheets prepared by 150 °C thermal annealing for 10 min were also determined. All of samples were spin-coated on ITO and tested in the same testing conditions. Figure 2a shows a rough morphology of the pristine MoS_2, and clearly stacked MoS_2 can be seen. However, Fig. 2b displays an individual MoS_2 sheet with six spot pattern in the selected-area electron diffraction (SAED) of MoS_2, suggesting that MoS_2 is scattered as individual MoS_2 nanosheet [38, 39]. Also, the severe aggregation of the pristine MoS_2 can be observed in SEM images (Fig. 2c), intriguingly, after being treated by ethyl cellulose ethanol solution via liquid ultrasound exfoliation, MoS_2 nanosheets can fully cover and tightly attach on the ITO substrate with a quite smooth surface morphology (Fig. 2d).

To further verify morphology results, the XRD patterns of pristine and exfoliated MoS_2 nanosheets (Fig. 3a)

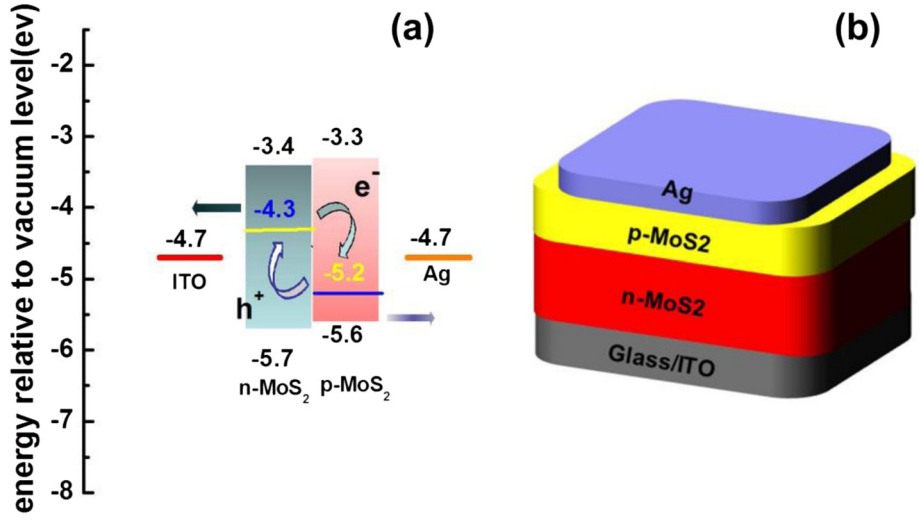

Fig. 5 a The schematic energy diagram of the MoS2 photodetector **b** the structure of MoS2 photodetector device

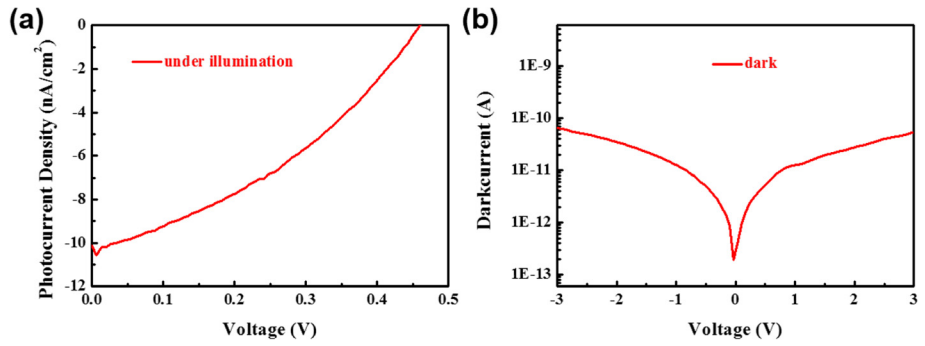

Fig. 6 Current-voltage curves of the device **a** under a 150-W Xe lamp light source illumination and **b** in dark

only the peaks of (103) and (002) plane remain after liquid exfoliation which confirms that the MoS_2 nanosheets were successfully striped [40, 41]. Moreover, the disappearance of other peaks could prove that ultrathin MoS_2 nanosheets are tightly deposited on the ITO glass with preferred ductility. The Raman spectrum can once again prove the exfoliation of MoS_2 nanosheets. The two peaks (1 and 2 g) between 360 and 430 cm^{-1} are the main peak of MoS_2 [42–44]. After liquid exfoliation, the obvious decrease of the intensity of the two peaks was observed.

It is well known that the MoS_2 nanosheets are n-type semiconductor materials and several researches have been reported that MoS_2 could be changed as a p-type semiconductor material with a relative high work function after UV-ozone plasma treatment. Thus, the properties of MoS_2 nanosheets with or without the UV-ozone plasma treatment were also investigated. Figure 4a is the X-ray photoelectron spectroscopy (XPS) profile of n-MoS_2 nanosheets (without plasma treatment) and p-MoS_2 nanosheets (with plasma treatment). The Mo 3D spectra of pristine MoS_2 nanosheets demonstrate outstanding $Mo^{4+}3d_{5/2}$ and $Mo^{4+}3d_{3/2}$ bands at 228.7 and 231.5 eV, in agreement with the other works for n-MoS_2 nanosheets. However, the two strong peaks have a notable shift to 235.3 and 232.5 eV, respectively, which is similar with the spectra of MoO_3 [45, 46]. Therefore, it proved that n-MoS_2 nanosheets can be successfully oxidized to p-type materials after UV-ozone plasma treatment. Since the MoS_2 layer is very thin via the spin-coating method, it is important to analyze the bilayer junction existing at the interface of n-MoS_2/p-MoS_2. To gain insight into the electronic structures of the n-MoS_2/p-MoS_2 bilayer junction, we have performed the UPS analysis. The work function was calculated through the difference between the cutoff of the highest binding energy and the photon energy of the exciting radiation. The valence band (VB) can be calculated from the cutoff from the lowest binding energy. As shown in Fig. 4b, after UV-ozone plasma treatment, the work function of the MoS_2 nanosheets has increased from 4.3 to 5.2 eV. The energy

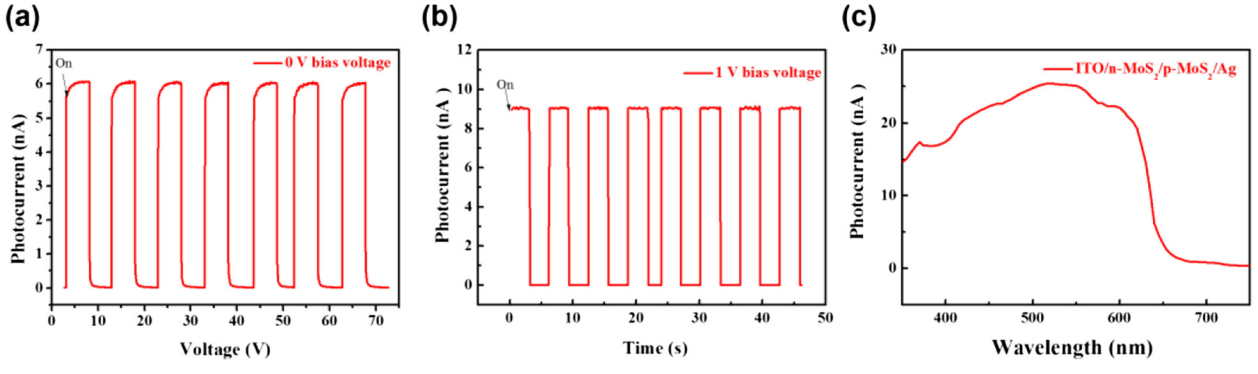

Fig. 7 **a** The output signal of photocurrent under alternating light on and light off, where the entire device was illuminated by a 150-W Xe lamp irradiation. Photoresponse of MoS_2-based photodetector at a 0-V DC bias voltage. **b** Photoresponse of MoS_2-based photodetector at 1-V DC bias voltage. **c** The spectral photoresponse vs. wavelength, showing a broad photoresponse range from 350 to 650 nm, which is, the absorption spectrum of the nanohybrid covers the whole energy range of visible light

difference between the Fermi level and valence band maximum is decreased from 1.4 to 0.4 eV, demonstrating the n-type MoS_2 nanosheets change to p-type MoS_2 nanosheets [47].

On the basis of the above results, we have constructed an energy diagram showing the band bending behavior at the n-MoS_2/p-MoS_2 bilayer junction interface, as shown in Fig. 5a. The n-MoS_2/p-MoS_2 bilayer junction with a built-in potential promises an excellent photodetector performance with a ITO/n-MoS_2/p-MoS_2/Ag device structure (Fig. 5b) which will be discussed later. The photocurrent-voltage curves and the photocurrent-voltage were measured with the Keithley 2400 source meter. As shown in Fig. 6a, b, the device shows the photovoltaic response under a 150-W Xe lamp light source illumination. The result shows the device have a p-n junction inside. In order to understand the photoelectric response properties in more detail and detect potential application in photoelectronic fields, we have performed further experiments of photodetector at a 1-V DC bias as shown in Fig. 7a, b. As seen from Fig. 7a, b, the photocurrent increases at an applied dc bias voltage of 0 and 1 V. Moreover, the photoresponse is steady, prompt, and reproducible during repeated on/off cycles of visible light illumination. More importantly, the n-MoS_2/p-MoS_2 bilayer junction-based device shows a very broad photoelectric response range from 350 to 600 nm, as shown in Fig. 7c, and therefore, the n-MoS_2/p-MoS_2 bilayer junction can harvest nearly the whole energy range of visible light.

Conclusions

We have demonstrated a high-quality n-MoS_2/p-MoS_2 bilayer junction-based device to achieve the high performance photoresponse which can harvest nearly the whole energy range of visible light. Excellent, thin exfoliated MoS_2 nanosheets are realized by a facile liquid exfoliation, changing the n-type MoS_2 nanosheets to p-type MoS_2 nanosheets via a simple plasma treatment. This work shows that thin MoS_2 nanosheets can be fully integrated into the photodetector manufacturing process, which holds promise for realizing 2D materials in a variety of optical electronic and optical devices.

Competing Interests

The authors declare that they have no competing interests.

Authors' Contributions

JY carried out the experiments. JY, XIL, JjZ, and QL participated in the design of the study. JY and XIL conceived of the study, participated in its design and coordination, and helped draft the manuscript. All authors read and approved the final manuscript.

Acknowledgements

This study was financially supported by the Natural Science Research Projects Funded of Anhui Colleges and Universities (KJ2015A224) and Scientific Research Fund of Anhui Province Education Department (KJ2010B104).

Author details

[1]Department of Chemistry and Environmental Engineering, Bengbu College, Bengbu, Anhui 233030, China. [2]School of Chemistry and Chemical Engineering, Hefei University of Technology, Hefei, Anhui 230009, China.

Received: 18 October 2015 Accepted: 17 November 2015
Published online: 25 November 2015

References

1. Eda G, Fujita T, Yamaguchi H, Voiry D, Chen M, Chhowalla M (2012) Coherent atomic and electronic heterostructures of single-layer MoS_2. ACS Nano 6:7311–7317
2. Eda G, Yamaguchi H, Voiry D, Fujita T, Chen M, Chhowalla M (2011) Photoluminescence from chemically exfoliated MoS_2. Nano Lett 11:5111–5116
3. Gu X, Cui W, Li H, Wu Z, Zeng Z, Lee ST, Zhang H, Sun B (2013) A solution-processed hole extraction layer made from ultrathin MoS_2 nanosheets for efficient organic solar cells. Adv Energy Mater 3:1262–1268
4. Wang QH, Kalantar-Zadeh K, Kis A, Coleman JN, Strano MS (2012) Electronics and optoelectronics of two-dimensional transition metal dichalcogenides. Nat Nanotechnol 7:699–712
5. Tan C, Liu Z, Huang W, Zhang H (2015) Non-volatile resistive memory devices based on solution-processed ultrathin two-dimensional nanomaterials. Chem Soc Rev 44:2615–2628
6. Tan C, Zhang H (2015) Two-dimensional transition metal dichalcogenide nanosheet-based composites. Chem Soc Rev 44:2713–2731
7. Huang X, Tan C, Yin Z, Zhang H (2014) 25th Anniversary article: hybrid nanostructures based on two-dimensional nanomaterials. Adv Mater 26:2185–2204
8. Huang X, Zeng Z, Zhang H (2013) Metal dichalcogenide nanosheets: preparation, properties and applications. Chem Soc Rev 42:1934–1946
9. Huang X, Yin Z, Wu S, Qi X, He Q, Zhang Q, Yan Q, Boey F, Zhang H (2011) Graphene-based materials: synthesis, characterization, properties, and applications. Small 7:1876–1902
10. Zhang H (2015) Ultrathin two-dimensional nanomaterials. ACS Nano 9:9451–9469
11. Huang X, Qi X, Boey F, Zhang H (2012) Graphene-based composites. Chem Soc Rev 41:666–686
12. Buscema M, Groenendijk DJ, Blanter SI, Steele GA, van der Zant HS, Castellanos-Gomez A (2014) Fast and broadband photoresponse of few-layer black phosphorus field-effect transistors. Nano Lett 14:3347–3352
13. Scalise E, Houssa M, Pourtois G, Afanas'ev V, Stesmans A (2012) Strain-induced semiconductor to metal transition in the two-dimensional honeycomb structure of MoS_2. Nano Res 5:43–48
14. Remskar M, Mrzel A, Virsek M, Godec M, Krause M, Kolitsch A, Singh A, Seabaugh A (2010) The MoS_2 nanotubes with defect-controlled electric properties. Nanoscale Res Lett 6:26
15. Yin Z, Li H, Li H, Jiang L, Shi Y, Sun Y, Lu G, Zhang Q, Chen X, Zhang H (2012) Single-layer MoS_2 phototransistors. ACS Nano 6:74–80
16. Yuwen L, Xu F, Xue B, Luo Z, Zhang Q, Bao B, Su S, Weng L, Huang W, Wang L (2014) General synthesis of noble metal (Au, Ag, Pd, Pt) nanocrystal modified MoS_2 nanosheets and the enhanced catalytic activity of Pd-MoS_2 for methanol oxidation. Nanoscale 6:5762–5769
17. Xu M, Liang T, Shi M, Chen H (2013) Graphene-like two-dimensional materials. Chem Rev 113:3766–3798
18. Radisavljevic B, Radenovic A, Brivio J, Giacometti V, Kis A (2011) Single-layer MoS_2 transistors. Nat Nanotechnol 6:147–150
19. Lopez-Sanchez O, Lembke D, Kayci M, Radenovic A, Kis A (2013) Ultrasensitive photodetectors based on monolayer MoS_2. Nat Nanotechnol 8:497–501
20. Shi H, Yan R, Bertolazzi S, Brivio J, Gao B, Kis A, Jena D, Xing HG, Huang L (2013) Exciton dynamics in suspended monolayer and few-layer MoS_2 2D crystals. ACS Nano 7:1072–1080
21. Wang H, Yu L, Lee Y-H, Shi Y, Hsu A, Chin ML, Li L-J, Dubey M, Kong J, Palacios T (2012) Integrated circuits based on bilayer MoS_2 transistors. Nano Lett 12:4674–4680
22. Conley HJ, Wang B, Ziegler JI, Haglund RF Jr, Pantelides ST, Bolotin KI (2013) Bandgap engineering of strained monolayer and bilayer MoS_2. Nano Lett 13:3626–3630

23. Bertolazzi S, Krasnozhon D, Kis A (2013) Nonvolatile memory cells based on MoS_2/graphene heterostructures. ACS Nano 7:3246–3252
24. Mak KF, He K, Shan J, Heinz TF (2012) Control of valley polarization in monolayer MoS_2 by optical helicity. Nat Nanotechnol 7:494–498
25. Lee Y-H, Yu L, Wang H, Fang W, Ling X, Shi Y, Lin C-T, Huang J-K, Chang M-T, Chang C-S (2013) Synthesis and transfer of single-layer transition metal disulfides on diverse surfaces. Nano Lett 13:1852–1857
26. Chen J-R, Odenthal PM, Swartz AG, Floyd GC, Wen H, Luo KY, Kawakami RK (2013) Control of Schottky barriers in single layer MoS_2 transistors with ferromagnetic contacts. Nano Lett 13:3106–3110
27. Li H, Wu J, Yin Z, Zhang H (2014) Preparation and applications of mechanically exfoliated single-layer and multilayer MoS_2 and WSe_2 nanosheets. Accounts Chem Res 47:1067–1075
28. Li H, Yin Z, He Q, Li H, Huang X, Lu G, Fam DWH, Tok AIY, Zhang Q, Zhang H (2012) Fabrication of single- and multilayer MoS_2 film-based field-effect transistors for sensing no at room temperature. Small 8:63–67
29. Li H, Lu G, Yin Z, He Q, Li H, Zhang Q, Zhang H (2012) Optical identification of single- and few-layer MoS_2 sheets. Small 8:682–686
30. Li H, Wu J, Huang X, Lu G, Yang J, Lu X, Xiong Q, Zhang H (2013) Rapid and reliable thickness identification of two-dimensional nanosheets using optical microscopy. ACS Nano 7:10344–10353
31. Lee HS, Min S-W, Chang Y-G, Park MK, Nam T, Kim H, Kim JH, Ryu S, Im S (2012) MoS_2 nanosheet phototransistors with thickness-modulated optical energy gap. Nano Lett 12:3695–3700
32. Yoon Y, Ganapathi K, Salahuddin S (2011) How good can monolayer MoS_2 transistors be? Nano Lett 11:3768–3773
33. Zeng Z, Yin Z, Huang X, Li H, He Q, Lu G, Boey F, Zhang H (2011) Single-layer semiconducting nanosheets: high-yield preparation and device fabrication. Angew Chem Int Edit 50:11093–11097
34. Liu J, Zeng Z, Cao X, Lu G, Wang L-H, Fan Q-L, Huang W, Zhang H (2012) Preparation of MoS_2-polyvinylpyrrolidone nanocomposites for flexible nonvolatile rewritable memory devices with reduced graphene oxide electrodes. Small 8:3517–3522
35. Viculis LM, Mack JJ, Mayer OM, Hahn HT, Kaner RB (2005) Intercalation and exfoliation routes to graphite nanoplatelets. J Mater Chem 15:974–978
36. Coleman JN, Lotya M, O'Neill A, Bergin SD, King PJ, Khan U, Young K, Gaucher A, De S, Smith RJ (2011) Two-dimensional nanosheets produced by liquid exfoliation of layered materials. Science 331:568–571
37. Hsu C-L, Tsai T-Y (2011) Fabrication of fully transparent indium-doped ZnO nanowire field-effect transistors on ITO/glass substrates. J Electrochem Soc 158:K20–K23
38. Fu W, Du F-H, Su J, Li X-H, Wei X, Ye T-N, Wang K-X, Chen J-S (2014) In situ catalytic growth of large-area multilayered graphene/MoS_2 heterostructures. Sci rep-UK 4:4673
39. Yu X, Prévot MS, Sivula K (2014) Multiflake thin film electronic devices of solution processed 2D MoS_2 enabled by sonopolymer assisted exfoliation and surface modification. Chem Mater 26:5892–5899
40. Zheng X, Xu J, Yan K, Wang H, Wang Z, Yang S (2014) Space-confined growth of MoS_2 nanosheets within graphite: the layered hybrid of MoS_2 and graphene as an active catalyst for hydrogen evolution reaction. Chem Mater 26:2344–2353
41. Nguyen EP, Carey BJ, Daeneke T, Ou JZ, Latham K, Zhuiykov S, Kalantar-Zadeh K (2014) Investigation of two-solvent grinding-assisted liquid phase exfoliation of layered MoS_2. Chem Mater 27:53–59
42. Terrones H, Del Corro E, Feng S, Poumirol J, Rhodes D, Smirnov D, Pradhan N, Lin Z, Nguyen M, Elias A (2014) New first order raman-active modes in few layered transition metal dichalcogenides. Sci Rep-UK 4:4215
43. Chen C, Qiao H, Lin S, Luk CM, Liu Y, Xu Z, Song J, Xue Y, Li D, Yuan J (2015) Highly responsive MoS_2 photodetectors enhanced by graphene quantum dots. Sci Rep-UK 5:11830
44. Wang S, Rong Y, Fan Y, Pacios M, Bhaskaran H, He K, Warner JH (2014) Shape evolution of monolayer MoS_2 crystals grown by chemical vapor deposition. Chem Mater 26:6371–6379
45. Varrla E, Backes C, Paton KR, Harvey A, Gholamvand Z, McCauley J, Coleman JN (2015) Large-scale production of size-controlled MoS_2 nanosheets by shear exfoliation. Chem Mater 27:1129–1139
46. Alov NV (2015) XPS study of MoO_3 and WO_3 oxide surface modification by low-energy Ar + ion bombardment. Phys Status Solidi C 12:263–266
47. Chuang S, Battaglia C, Azcatl A, McDonnell S, Kang JS, Yin X, Tosun M, Kapadia R, Fang H, Wallace RM (2014) MoS_2 p-type transistors and diodes enabled by high work function MoO_x contacts. Nano Lett 14:1337–1342